IEEE Photonics Journal
An IEEE Photonics Society Publication

Open Access

Tunable Q-Switched Fiber Laser Based on a Graphene Saturable Absorber Without Additional Tuning Element

Volume 11, Number 1, February 2019

Renli Zhang
Jun Wang
Meisong Liao
Xia Li
Pei-Wen Kuan
Yinyao Liu
Yan Zhou
Weiqing Gao

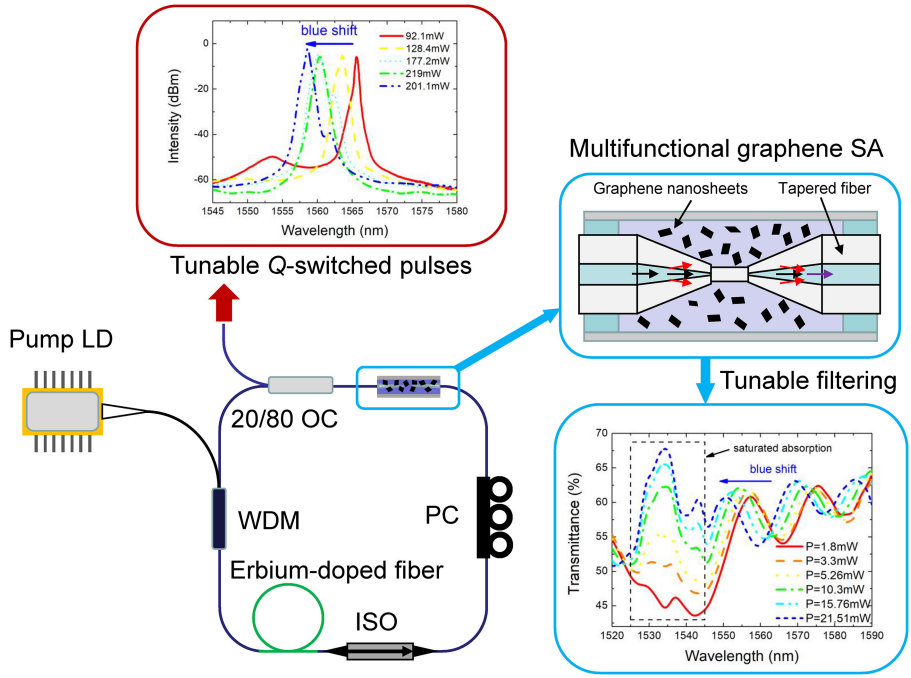

DOI: 10.1109/JPHOT.2019.2892646

Tunable Q-Switched Fiber Laser Based on a Graphene Saturable Absorber Without Additional Tuning Element

Renli Zhang,[1,2] **Jun Wang**,[1] **Meisong Liao**,[1] **Xia Li**,[1] **Pei-Wen Kuan**,[1] **Yinyao Liu**,[1] **Yan Zhou**,[3] **and Weiqing Gao**[4]

[1]Key Laboratory of Materials for High Power Laser, Shanghai Institute of Optics and Fine Mechanics, Chinese Academy of Sciences, Shanghai 201800, China
[2]Center of Materials Science and Optoelectronics Engineering, University of Chinese Academy of Sciences, Beijing 100049, China
[3]College of Science, Shanghai Institute of Technology, Shanghai 201418, China
[4]School of Electronic Science & Applied Physics, Hefei University of Technology, Hefei 230009, China

DOI:10.1109/JPHOT.2019.2892646

Manuscript received December 6, 2018; revised December 24, 2018; accepted January 9, 2019. Date of publication January 16, 2019; date of current version January 31, 2019. This work was supported in part by the National Key Research and Development Program of China under Grant 2018YFB0504500, in part by the National Natural Science Foundation of China under Grants 61475171, 61705244, 61307056, and 61875052, and in part by the Natural Science Foundation of Shanghai under Grants 17ZR1433900 and 17ZR1434200. Corresponding author: Meisong Liao (e-mail: liaomeisong@siom.ac.cn).

Abstract: A tunable passively *Q*-switched fiber laser is fabricated using a graphene saturable absorber. The graphene saturable absorber is composed of a tapered fiber coated with graphene nanosheets. It combines the abilities of a saturable absorber and power-dependent tunable filter, thereby simplifying the structure of the tunable passively *Q*-switched fiber laser. The transmission peak of the graphene saturable absorber is linearly dependent on the input power and temperature, with slopes of approximately −0.35 nm/mW and −3.63 nm/°C, respectively. The *Q*-switched fiber laser exhibits a tunable wavelength range of 7 nm (from 1558 to 1565 nm). The output pulse offers the shortest pulse duration of 2.22 μs with a repetition rate of 39.1 kHz and the widest pulse duration is 5.9 μs that corresponds to a repetition rate of 21.3 kHz. The maximum pulse energy is 251.9 nJ, corresponding to an average output power of 8.6 mW.

Index Terms: Graphene, saturable absorber, wavelength tunable operation, Q-switched fiber lasers.

1. Introduction

Q-switched erbium-doped fiber lasers have been widely applied in diverse fields such as laser processing, remote sensing, medicine and telecommunications [1], [2]. According to the type of *Q*-factor switching, *Q*-switched fiber lasers can be classified as either passive or active. Compared to the actively *Q*-switched fiber lasers, which need additional external switching electronics, passively *Q*-switched fiber lasers have attracted more attention owing to their advantages of compactness, low cost, and simple configurations [3]–[5]. The saturable absorber (SA) is a key element for the passively *Q*-switched fiber laser, as it is quite important for the *Q*-switching output perfor-

mance. The most commonly used SA for a passively *Q*-switched fiber laser is a semiconductor saturable absorber mirror (SESAM). However, the SESAM has drawbacks such as a low damage threshold and small response bandwidth, which limit its applications in passively *Q*-switched fiber lasers [4], [6].

In recent years, graphene, a new type of two-dimensional (2D) material, has generated significant interest for pulse lasers. Compared to other 2D materials, graphene offers outstanding properties, including a fast recovery time, large response bandwidth, and simple fabrication [7]–[12]. Since the discovery of graphene, extensive studies have been conducted on passively *Q*-switched fiber lasers using graphene SAs [1], [4], [13]–[20]. In particular, graphene-based tunable *Q*-switched fiber lasers are incredibly attractive systems in this field. Compared to the SESAM, graphene provides a large response bandwidth and good thermal conductivity, making it beneficial to the generation of wavelength-tunable pulses with high pulse energies [4].

There are several reports on tunable *Q*-switched fiber lasers using graphene SAs [2]–[5], [21]. In 2011, a tunable *Q*-switched fiber laser was realized using a graphene-film SA and tunable filter that covered a tunable wavelength range of 32 nm [4]. In 2013, Ahmad *et al.* reported a graphene tunable *Q*-switched fiber laser based on a tunable fiber Bragg grating, which provided a tunable range of 10 nm [2]. All the reported graphene tunable *Q*-switched fiber lasers need additional tuning elements such as a tunable bandpass filter [3]–[5], [21] or tunable fiber Bragg grating [2], which increase the complexity of the laser system. Compared to the graphene-film SA used in the reported tunable *Q*-switched fiber laser, graphene SAs based on tapered fibers provide advantages of a high damage threshold, large interaction length, and simplicity to modularize and package [22]. Moreover, owing to the multimode interference, tapered fibers can provide wavelength-dependent transmissions and used as tunable filters in tunable fiber lasers [23], [24]. Therefore, it can be expected that a tapered fiber coated with graphene can be used as both tuning element and SA in the tunable passively *Q*-switched fiber laser, thereby reducing the complexity and cost of the tunable fiber laser.

In this study, a multifunctional graphene SA that could be used as both a saturable absorber and tunable filter has been reported for the first time. With this multifunctional graphene SA, a tunable *Q*-switched fiber laser was demonstrated that did not use any additional tuning element. The multifunctional graphene SA is composed of a tapered fiber coated with graphene. The transmission peak wavelength of the graphene SA was found to be linearly dependent on the temperature and input power, with slopes of approximately -3.63 nm/°C and -0.35 nm/mW, respectively. Unlike the previous works [24]–[26], the present tunable laser used temperature-dependent filtering property of a tapered fiber to achieve tunable wavelength controlled by pump power. Owing to the tunable filtering property of the multifunctional graphene SA, the configuration of the tunable laser was simplified. To the best of our knowledge, this is the first demonstration of a tunable graphene-based *Q*-switched fiber laser without an additional tuning element.

In these experiments, the *Q*-switched fiber laser had a tunable wavelength range of 7 nm (from 1558 to 1565 nm), with a maximum pulse energy of 251.9 nJ and signal–to–noise ratio of 48 dB. The high pulse energy, stable pulse output, and simple configuration implied that this tunable *Q*-switched fiber laser was suitable for use as a seed in a master oscillator power-amplifier (MOPA) system in practical applications.

2. Fabrication and Characterization of the Graphene SA

The graphene nanosheets used in our experiment were purchased from a chemical manufacturer (XFNANO, Nanjing, China). According to the information provided by the manufacturer, the diameter and thickness of the graphene nanosheets were 5–10 μm and 3–10 nm, respectively. Considering the height of the monolayer graphene to be 0.33 nm, the number of layers of the graphene nanosheets was estimated as 9–30.

The tapered fiber was fabricated by an oxyhydrogen-flame stretching method with a segment of a single-mode fiber (SMF-28). The waist diameter of the tapered fiber was approximately 4.8 μm and the length of the waist region was $\sim$2.5 mm. The measured intrinsic loss was 0.03 dB at

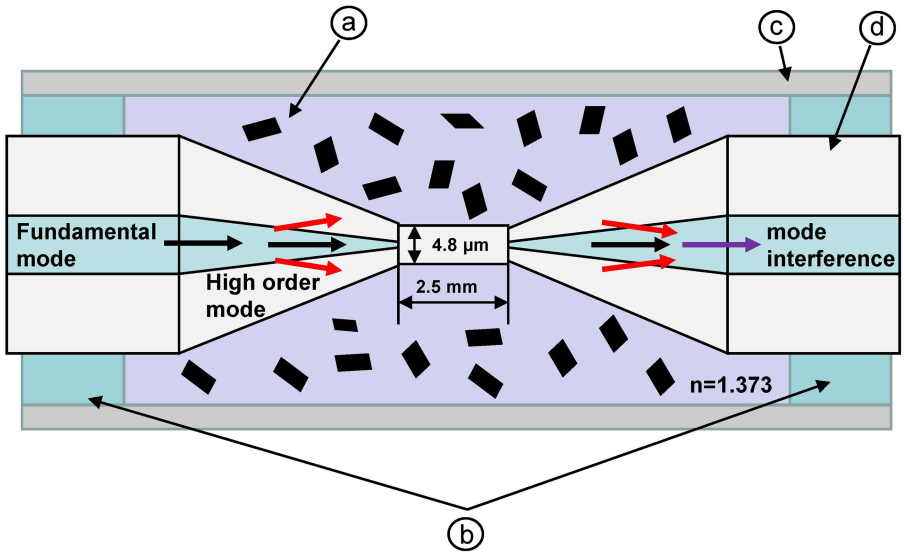

Fig. 1. Schematic illustration of the graphene SA based on a tapered fiber (a: UV-curing adhesive mixed with graphene nanosheets, b: UV-curing adhesive used to fix the tapered fiber, c: U groove, and d: tapered fiber).

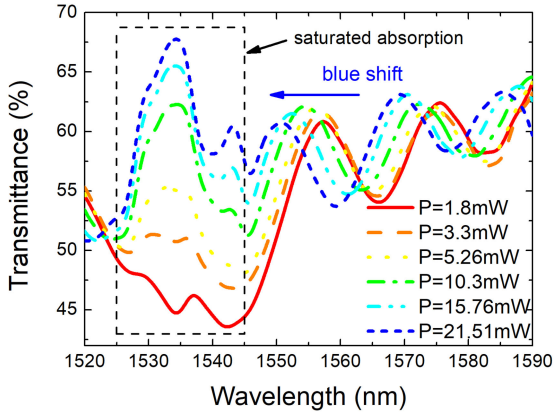

Fig. 2. Transmission spectra of the graphene SA under different input powers (red solid line: 1.8 mW, orange dashed line: 3.3 mW, yellow dotted line: 5.26 mW, green dash–dot line: 10.3 mW, cyan dash–dot–dot line: 15.76 mW, and blue short-dash line: 21.51 mW).

1550 nm. The tapered fiber was fixed in a silica glass U groove for the following treatment. Graphene nanosheets (20 mg) were mixed with an ultraviolet (UV)-curing adhesive with a refractive index of 1.373. To ensure a sufficiently high concentration and good packaging effect, the mass ratio of graphene nanosheets and UV-curing adhesive was determined to be 1:100. The obtained mixture was poured into the U groove and completely covered the tapered fiber. After 10 s of UV irradiation, the mixture was solidified in the U groove and the simply packaged graphene SA was obtained. A schematic illustration of the graphene SA is shown in Fig. 1.

The tapered fiber could provide a wavelength-dependent transmission owing to mode interference [23], [25]. The linear transmission spectrum of the present graphene SA was measured using a home-made amplified spontaneous emission (ASE) source. The measurement was repeated several times, yielding consistent results. The measured results are shown in Fig. 2. The transmission spectrum showed a peak (∼1558 nm) in the wavelength range of 1540 to 1565 nm. When the input power is increased from 1.8 to 21.51 mW, the peak wavelength of the transmission spectrum is shifted from 1558 to 1550.8 nm. The wavelength shift was approximately 7 nm with an input power

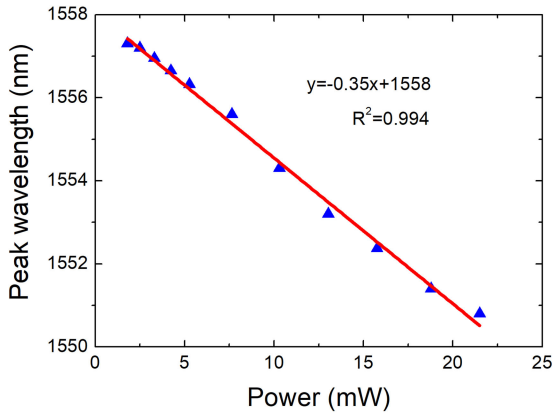

Fig. 3. Transmission peak wavelength of the graphene SA as a function of the input power.

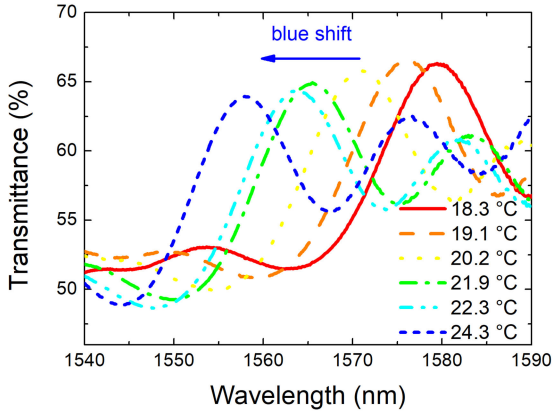

Fig. 4. Transmission spectra of the graphene SA at different temperatures (red solid line: 18.3 °C, orange dashed line: 19.1 °C, yellow dotted line: 20.2 °C, green dash–dot line: 21.9 °C, cyan dash–dot–dot line: 22.3 °C, and blue short-dash line: 24.3 °C).

increment of approximately 19.7 mW. Moreover, the transmittance between 1525 nm and 1545 nm increased with the input power. This could be attributed to the saturable absorption of the graphene SA. The intensity of the ASE spectrum peak (∼1535 nm) significantly increased with the increase in power, leading to light absorption saturation between 1525 nm and 1545 nm. The transmission spectra in Fig. 2 were measured at a temperature of approximately 23 °C. The relationship between the peak wavelength of the transmission spectrum and input power of the ASE source is shown in Fig. 3; a linear relationship was observed with a slope of −0.35 nm/mW.

This input-power-dependent blue-shift could be attributed to the temperature increase on light absorption by the graphene nanosheets [28], [29]. The change in temperature influenced the refractive index of the surrounding media, leading to changes in the transmission spectrum [27]–[29]. For a detailed analysis of the temperature-dependent transmission spectrum, the graphene SA was placed on a temperature-controlled board. The transmission spectra of the graphene SA at different temperatures were measured with an input power of 0.08 mW, as shown in Fig. 4. When the temperature of the temperature-controlled board is increased from 18.3 to 24.3 °C, the transmission peak of the graphene SA is shifted to shorter wavelengths, with a wavelength shift of 21.7 nm, corresponding to a slope of approximately −3.63 nm/°C, as shown in Fig. 5.

The transmission spectrum of the tapered-fiber-based graphene SA was dependent on the size of the tapered fiber and refractive index of the media surrounding the tapered fiber [23]. By increasing the waist diameter of the tapered fiber and refractive index of the UV-curing adhesive, the

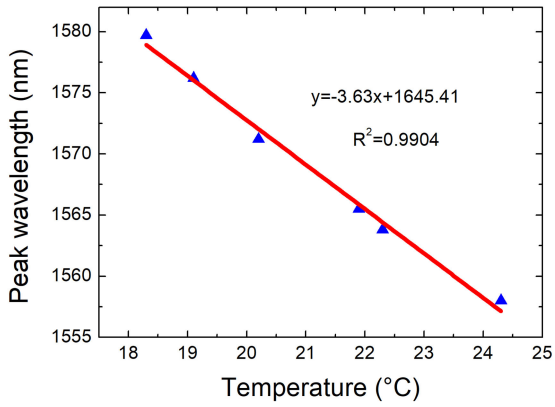

Fig. 5. Transmission peak wavelength of the graphene SA as a function of the temperature.

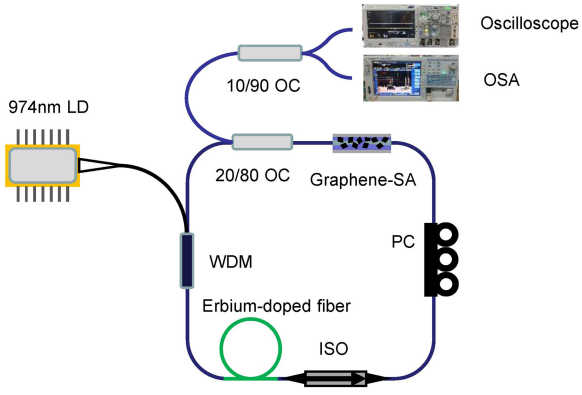

Fig. 6. Experimental setup of the passively *Q*-switched fiber laser using the graphene SA.

bandwidth of the transmission spectrum could be increased [23], which adjusted the filtering effect of the graphene SA. Moreover, owing to the influence of the absorption of light field by graphene nanosheets on the temperature of the graphene SA, the sensitivity of the wavelength shift to the input power could be altered by varying the concentration of graphene nanosheets mixed with the UV-curing adhesive. It can be expected that with a higher concentration of graphene nanosheets, the graphene SA could exhibit a larger temperature change under the same input power, providing a larger tuning range.

The nonlinear absorption of the graphene SA was measured using a passively erbium-doped mode-locked fiber laser with a pulse duration of 200 fs. The modulation depth of the graphene SA was measured to be 5.6%. However, owing to the effect of the power-dependent tuning, the measured modulation depth was only a rough result. In addition, during the measurement, the maximum input power was increased to 65 mW (corresponding to an intensity of $\sim$8.3 GW/cm^2) while the graphene SA was still undamaged. Therefore, the damage threshold of the graphene SA was at least higher than $\sim$8.3 GW/cm^2.

3. Experimental Setup of a Tunable *Q*-Switched Fiber Laser Using the Graphene SA

A passively *Q*-switched fiber laser using the graphene SA was constructed, as shown in Fig. 6. The pump source was a laser diode with a peak wavelength of 974 nm. The laser diode was connected

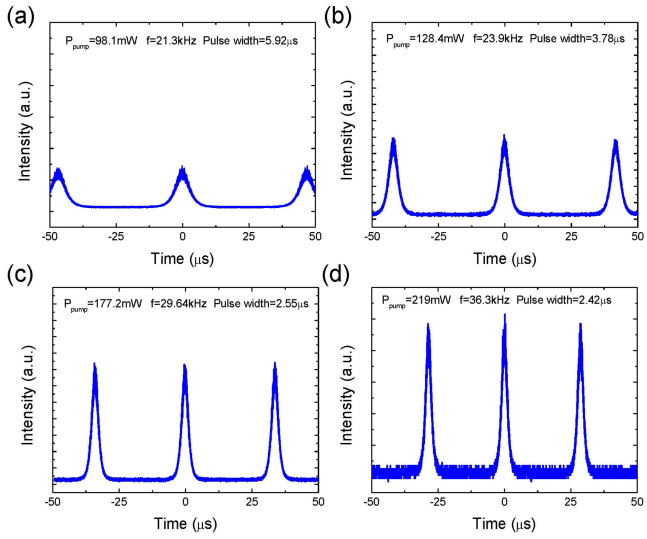

Fig. 7. *Q*-switched pulse trains under pump powers of (a) 98.1, (b) 128.4, (c) 177.2, and (d) 219 mW.

into the laser cavity through a 980/1550 wavelength division multiplexer (WDM). An approximately 0.65 m long erbium-doped fiber (Nufern SM-ESF-7/125) was spliced with the 1550 arm of the WDM. After the erbium-doped fiber, a polarization-independent isolator (ISO) was applied to ensure unidirectional operation. A polarization controller (PC) was used controlling the cavity polarization. The output pulse was coupled out of the cavity using the 20% fiber of a 20/80 output coupler (OC). The rest of the cavity was a single-mode fiber (SMF-28). The total length of the laser cavity was approximately 9.2 m. The 20% fiber of the 20/80 OC was connected to a 10/90 OC to divide the output signal into two signals. The laser performance was simultaneously detected by a digital oscilloscope (Tektronic MDO 3102) and optical spectrum analyzer (OSA Yokogawa AQ6370C).

4. Results and Discussion

When the pump power reached 92.1 mW, a stable *Q*-switched pulse was obtained. With the increase in the pump power, the laser continued to operate in the *Q*-switched regime, with increased output power and repetition rate. When the pump power increased to 183.1 mW, the *Q*-switched pulse disappeared. With a small adjustment of the PC, a stable *Q*-switched pulse was obtained again. With further increase in the pump power to 207 mW, the *Q*-switched pulse vanished again and reappeared with a proper adjustment of the PC. When the pump power exceeded 248 mW, the *Q*-switched pulse train disappeared and could not be restored even with a full-range adjustment of the PC. The output pulse trains under different pump powers are shown in Fig. 7.

As shown in Fig. 8, with the increase in the pump power, the repetition rate varied from 20.1 to 39.1 kHz. Meanwhile, the pulse width decreased with the increase of the pump power. The shortest pulse duration was 2.22 μs, corresponding to a repetition rate of 39.1 kHz. The widest pulse duration was 5.9 μs, corresponding to a repetition rate of 21.3 kHz. The relationships between the pulse width, repetition rate, and pump power are determined by the generation mechanism of *Q*-switched pulses. As the pump power increased, more gain was provided to saturate the SA, therefore shortening the pulse width and pulse period [4]. Figure 9 shows the output power and calculated pulse energy in the ranges of 2.1 to 9.2 mW and 119.3 to 251.9 nJ, respectively. The output power was calculated using the measured power at the 90% fiber of the 10/90 OC.

Figure 10(a) shows the typical *Q*-switched pulse when the laser operates under the pump power of 248 mW. The RF spectrum was measured with a resolution bandwidth (RBW) of 30 Hz, as shown in Fig. 10(b). The measured signal–to–noise ratio (SNR) was 48 dB, demonstrating the

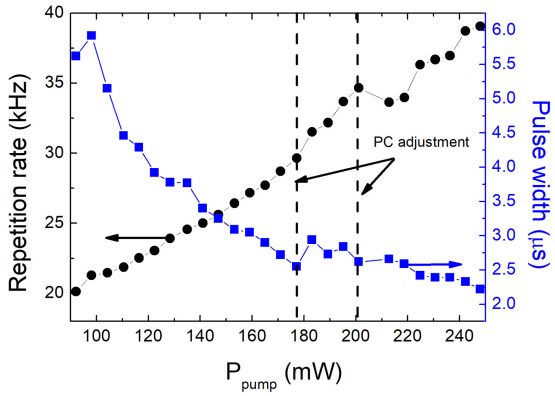

Fig. 8. Repetition rate and pulse width as a function of the pump power (black circles: repetition rate; blue squares: pulse width).

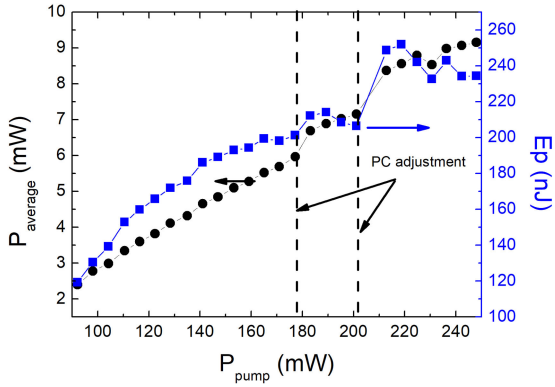

Fig. 9. Measured output power and calculated pulse energy as a function of the pump power (black circles: output power; blue squares: pulse energy).

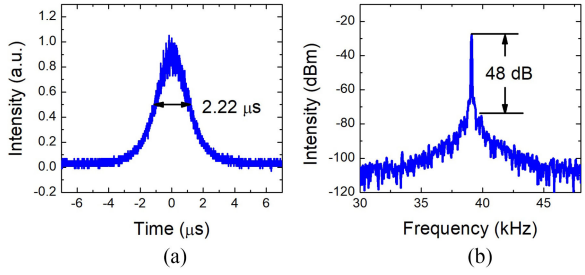

Fig. 10. (a) *Q*-switched pulse and (b) radio-frequency (RF) spectrum under the maximum pump power of 248 mW.

stable operation of the *Q*-switched fiber laser. To confirm the long-term stability of the fiber laser, the output power under a pump power of 248 mW was measured for an hour. The fluctuation of the output power was ∼5%, indicating a relatively good long-term stability of the fiber laser.

The output spectra under different pump powers are shown in Fig. 11. The increase in the pump power led to a blue-shift of the output spectrum with a tuning range of 7 nm, from 1565.6 to 1558.6 nm. The central wavelength of the output spectrum as a function of the pump power is shown in Fig. 12. Before the second adjustment of the PC, the pump power increased from 92.1 to 201.1 mW, leading to a wavelength shift from 1565.6 to 1558.6 nm. After the second adjustment of the PC, the *Q*-switched pulse reappeared with a central wavelength of 1560.8 nm. With further increase in the pump power, the blue-shift could still be observed, from 1560.8 to 1558.8 nm.

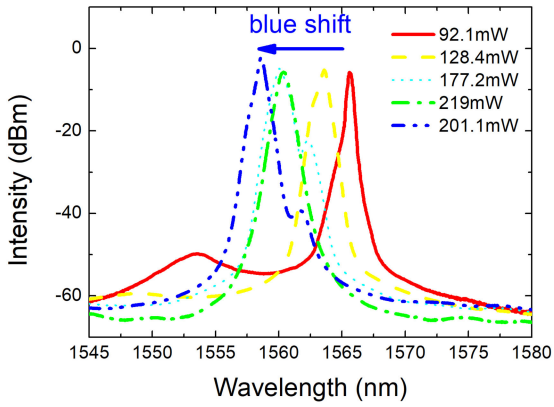

Fig. 11. Spectra of the output *Q*-switched pulses under different pump powers (red solid line: 92.1 mW, yellow dashed line: 128.4 mW, cyan dotted line: 177.2 mW, green dash–dot line: 201.1 mW, and blue dash–dot–dot line: 219 mW).

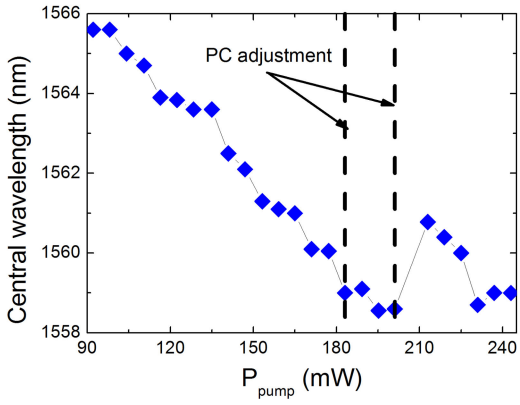

Fig. 12. Central wavelength of the output spectrum as a function of the pump power.

In the experiment, the change in temperature is originated from the absorption of light by graphene nanosheets distributed near the waist of the tapered fiber. Therefore, the temperature change of the tapered fiber could not be directly detected. In addition, during the experiment, the surface temperature of the graphene SA remained approximately constant; therefore, the temperature of the tapered fiber could not be obtained from the surface temperature. However, according to the slope of −3.63 nm/°C in Fig. 5, when the pump power increased from 92.1 to 183.1 mW (before the first adjustment of PC), the estimated temperature change was approximately 1.8 °C, corresponding to a tuning range of 6.6 nm.

According to the above results, the present *Q*-switched fiber laser provides a stable *Q*-switched operation with high-energy pulses and tuning ability with a simple configuration, making it suitable as a seed in a *Q*-switched fiber laser system based on a MOPA. The multifunctional graphene SA used in the present tunable *Q*-switched fiber laser was simple in structure and convenient to manufacture. Further studies on practical applications can be expected in the future.

In addition, a passive mode-locking operation using the graphene SA was also attempted. During the experiment, with the proper adjustment of the PC, mode-locking operation was realized. However, the stability of the mode-locking pulse was not good enough. The SNR of the mode-locking pulse was only 30–40 dB. The reason may be that the distance between the graphene nanosheets dispersed in the adhesive and tapered fiber was too large, resulting in a poor mode-locking performance. In general, the performance of the graphene SA has great potential for improvement. To

TABLE 1
Output Performances of Tunable Erbium-Doped *Q*-Switched Fiber Lasers Incorporating Graphene Saturable Absorbers

Reference	Pulse width (μ s)	Maximum pulse energy (nJ)	Repetition rate (kHz)	Tunable range (nm)	Additional tuning element
[2]	0.412	16.26	1.387-208	10	TFBG
[3]	1.52	106.2	5-45	46	Tunable filter
[4]	2	40	36-103	32	Tunable filter
[5]	1.6	25.8	18.9-55.3	58	Tunable filter
[21]	2.6	1050	7.5-25.5	16	Tunable filter
[30]	2.22	33.8	24.3-39.1	9.84	SMS filter
This work	13.6	251.9	20.1-39.1	7	None

TFBG stands for tunable fiber Bragg grating and SMS refers to single mode–multimode–single mode fiber.

further improve its performance, it is necessary to establish a theoretical model in the future. More theoretical and practical works are needed in upcoming research.

The output performances of previously reported tunable *Q*-switched fiber lasers using graphene SAs are listed in Table 1. The output details of this work are presented at the bottom of the list. With no additional tuning element, comparable results were obtained in our tunable *Q*-switched fiber laser.

5. Conclusion

In this article, a tunable passively *Q*-switched fiber laser using a tapered-fiber-based graphene SA was demonstrated. Owing to the multimode interference and temperature-dependent refractive index of the surrounding media, the graphene SA provided a temperature-dependent tunable transmission spectrum. The transmission peak of the graphene saturable absorber was found to be linearly dependent on the input power and temperature, with slopes of approximately -0.35 nm/mW and -3.63 nm/°C, respectively. Based on the graphene SA with a tunable filter, a tunable passively *Q*-switched fiber laser was constructed without any additional tuning element. The *Q*-switched pulse obtained in the experiment had a repetition rate in the range of 20.1 to 39.1 kHz. The shortest pulse duration was 2.22 μs, corresponding to a repetition rate of 39.1 kHz. The widest pulse duration was 5.9 μs, corresponding to a repetition rate of 21.3 kHz. The maximum pulse energy was 251.9 nJ. With the increase in the pump power, the operating wavelength shifted from 1565.6 to 1558.6 nm, providing a tuning range of 7 nm. The graphene SA with a tunable filter simplifies the configuration of the tunable *Q*-switched fiber laser. To the best of our knowledge, this is the first demonstration of a tunable graphene-based *Q*-switched fiber laser without an additional tuning element.

References

[1] L. Wei, D.-P. Zhou, H. Y. Fan, and W.-K. Liu, "Graphene-based *Q*-switched erbium-doped fiber laser with wide pulse-repetition-rate range," *IEEE Photon. Technol. Lett.*, vol. 24, no. 4, pp. 309–311, Feb. 2012.
[2] H. Ahmad, M. Z. Zulkifli, F. D. Muhammad, A. Z. Zulkifli, and S. W. Harun, "Tunable graphene-based *Q*-switched erbium-doped fiber laser using fiber Bragg grating," *J. Mod. Opt.*, vol. 60, no. 3, pp. 202–212, 2013.

[3] D.-P. Zhou, L. Wei, and W.-K. Liu, "Tunable graphene *Q*-switched erbium-doped fiber laser with suppressed self-mode locking effect," *Appl. Opt.*, vol. 51, no. 14, pp. 2554–2558, May. 2012.
[4] D. Popa, Z. Sun, T. Hasan, F. Torrisi, F. Wang, and A. C. Ferrari, "Graphene *Q*-switched, tunable fiber laser," *Appl. Phys. Lett.*, vol. 98, no. 7, Feb. 2011, Art. no. 073106.
[5] H. Ahmad, F. D. Muhammad, M. Z. Zulkifli, and S. W. Harun, "Wideband tunable *Q*-switched fiber laser using graphene as a saturable absorber," *J. Mod. Opt.*, vol. 60, no. 18, pp. 1563–1568, 2013.
[6] Z. Kang *et al.*, "Passively *Q*-switched erbium doped fiber laser using a gold nanostars based saturable absorber," *Photon. Res.*, vol. 6, no. 6, pp. 549–553, Jun. 2018.
[7] G. Xing, H. Guo, X. Zhang, T. C. Sum, and C. H. A. Huan, "The physics of ultrafast saturable absorption in graphene," *Opt. Exp.*, vol. 18, no. 5, pp. 4564–4573, Mar. 2010.
[8] A. Martinez and Z. Sun, "Nanotube and graphene saturable absorbers for fibre lasers," *Nature Photon.*, vol. 7, no. 11, pp. 842–845, Nov. 2013.
[9] Z. Sun and T. Hasan, "Graphene mode-locked ultrafast laser," *ACS Nano*, vol. 4, no. 2, pp. 803–810, Feb. 2010.
[10] Z. T. Wang, Y. Chen, C. J. Zhao, H. Zhang, and S. C. Wen, "Switchable dual-wavelength synchronously *Q*-switched erbium-doped fiber laser based on graphene saturable absorber," *IEEE Photon. J.*, vol. 4, no. 3, pp. 869–876, Jun, 2012.
[11] J. Ma *et al.*, "Few-layer black phosphorus based saturable absorber mirror for pulsed solid-state lasers," *Opt. Exp.*, vol. 23, no. 17, pp. 22643–22648, 2015.
[12] X. Jiang *et al.*, "Broadband nonlinear photonics in few-layer MXene $Ti_3C_2T_x$ (T = F, O, or OH)," *Laser Photon. Rev.*, vol. 12, no. 2, 2018, Art. no. 1700229.
[13] Z. Luo *et al.*, "Graphene-based passively *Q*-switched dual-wavelength erbium-doped fiber laser," *Opt. Lett.*, vol. 35, no. 21, pp. 3709–3711, Nov. 2010.
[14] H. Ahmad *et al.*, "Passively *Q*-switched 11-channel stable brillouin erbium-doped fiber laser with graphene as the saturable absorber," *IEEE Photon. J.*, vol. 4, no. 5, pp. 2050–2056, Oct. 2012.
[15] J. Wang *et al.*, "Evanescent-light deposition of graphene onto tapered fibers for passive *Q*-switch and mode-locker," *IEEE Photon. J.*, vol. 4, no. 5, pp. 1295–1305, Oct. 2012.
[16] Z. Wang *et al.*, "Multilayer graphene for *Q*-switched mode-locking operation in an erbium-doped fiber laser," *Opt. Commun.*, vol. 300, no. 14, pp. 17–21, 2013.
[17] Z. T. Wang *et al.*, "Graphene sheet stacks for *Q*-switching operation of an erbium-doped fiber laser," *Laser Phys. Lett.*, vol. 10, no. 7, Jul. 2013, Art. no. 075102.
[18] Y. Tang, X. Yu, X. Li, Z. Yan, and Q. J. Wang, "High-power thulium fiber laser *Q* switched with single-layer graphene," *Opt. Lett.*, vol. 39, no. 3, pp. 614–617, Feb. 2014.
[19] D. Wu *et al.*, "Passive synchronization of 1.06- and 1.53-mm fiber lasers *Q*-switched by a common graphene SA," *IEEE Photon. Technol. Lett.*, vol. 26, no. 14, pp. 1474–1477, Jul. 2014.
[20] F. Zhao, Y. Wang, Y. Wang, H. Wang, and Y. Cai, "Graphene oxide-COOH as a new saturable absorber for both *Q*-switching and mode-locking fiber lasers," *Chin. Opt. Lett.*, vol. 15, no. 10, 2017, Art. no. 101402.
[21] D. Wu *et al.*, "Large-energy, wavelength-tunable, all-fiber passively *Q*-switched Er: Yb-codoped double-clad fiber laser with mono-layer chemical vapor deposition graphene," *Appl. Opt.*, vol. 53, no. 19, pp. 4089–4093, Jul. 2014.
[22] K. Wu *et al.*, "High-performance mode-locked and *Q*-switched fiber lasers based on novel 2D materials of topological insulators, transition metal dichalcogenides and black phosphorus: review and perspective (invited)," *Opt. Commun.*, vol. 406, pp. 214–229, 2018.
[23] D. T. Cassidy, D. C. Johnson, and K. O. Hill, "Wavelength-dependent transmission of monomode optical fiber tapers," *Appl. Opt.*, vol. 24, no. 7, pp. 945–950, Apr. 1985.
[24] K. Kieu and M. Mansuripur, "Tuning of fiber lasers by use of a single-mode biconic fiber taper," *Opt. Lett.*, vol. 31, no. 16, pp. 2435–2437, 2006.
[25] J. H. Chen *et al.*, "Microfiber-coupler-assisted control of wavelength tuning for *Q*-switched fiber laser with few-layer molybdenum disulfide nanoplates," *Opt. Lett.*, vol. 40, no. 15, pp. 3576–3579, 2015.
[26] H. Ahmad, M. J. Faruki, Z. C. Tiu, and K. Thambiratnam, "Sub-nanometer tuning of mode-locked pulse by mechanical strain on tapered fiber," *Opt. Commun.*, vol. 387, pp. 84–88, 2017.
[27] W. Lin *et al.*, "Laser-induced thermal effect for tunable filter employing ferrofluid and fiber taper coupler," *IEEE Photon. Technol. Lett.*, vol. 27, no. 22, pp. 2339–2342, Nov. 2015.
[28] Z. Yang *et al.*, "Refractive index and temperature sensing characteristics of an optical fiber sensor based on a tapered single mode fiber/polarization maintaining fiber," *Chin. Opt. Lett.*, vol. 14, no. 5, 2016, Art. no. 050604.
[29] R. Yang *et al.*, "A highly sensitive temperature sensor based on a liquid-sealed S-tapered fiber," *IEEE Photon. Technol. Lett.*, vol. 25, no. 9, pp. 829–832, May. 2013.
[30] H. Ahmad, A. Z. Zulkifli, and K. Thambiratnam, "Tunable *Q*-switched erbium-doped fiber laser based on curved multimode fiber and graphene oxide saturable absorber," *Laser Phys.*, vol. 27, no. 5, 2017, Art. no. 055103.